

A New Method for Resolving Combinatorial Ambiguities at Hadron Colliders

Arvind Rajaraman* and Felix Yu†

Department of Physics and Astronomy,

University of California, Irvine, CA 92697-4575, USA

(Dated: September 14, 2010)

Abstract

We present a new method for resolving combinatorial ambiguities that arise in multi-particle decay chains at hadron colliders where the assignment of visible particles to the different decay chains has ambiguities. Our method, based on selection cuts favoring high transverse momentum and low invariant mass pairings, is shown to be significantly superior to the more traditional hemisphere method for a large class of decay chains, producing an increase in signal retention of up to a factor of 2. This new method can thus greatly reduce the combinatorial ambiguities of decay chain assignments.

PACS numbers: 13.85.-t

* arajaram@uci.edu

† felixy@uci.edu

I. INTRODUCTION

The turn-on of the Large Hadron Collider ushers in a data-driven era of particle physics. Major theoretical frameworks, such as supersymmetry (SUSY) and universal extra dimensions (UED), will be tested using present and upcoming collider data. In many such models, the lightest new physics particle is protected from decaying into Standard Model particles because of a discrete symmetry, e.g. R -parity or Kaluza-Klein parity for SUSY and UED, respectively. The resulting lightest supersymmetric particle (LSP) or lightest KK-odd particle (LKP), if neutral, is usually a viable dark matter candidate.

Measuring the properties of this dark matter candidate is critical for determining its cosmological behavior and its ultimate suitability as the dark matter. Because of the discrete symmetry, these particles must be produced in pairs at colliders, but since they escape, they manifest themselves in a collider event as large amounts of missing transverse momentum. Since only the total missing transverse momentum can be measured, the kinematics of these events cannot be fully reconstructed, and as a result, the dark matter candidate mass cannot in general be measured in any given event. It is therefore important to have methods of measuring this mass, which also serves to set the overall scale of new physics.

A large number of kinematic analysis techniques have been proposed in the literature to extract the mass of the dark matter candidate. Broadly speaking, these can be divided into three categories. The first is based on edge measurements of invariant mass distributions, using the fact that the algebraic expressions for such endpoints are related to the on-shell masses of the cascade decay chain [1–9]. The second class of analysis methods is known as the polynomial method, which solves the non-linear kinematic four-momentum conservation equations and thus determines the masses of the entire decay chain [10–14]. The last broad category of approaches uses new kinematic observables and functions such as m_{T2} , m_{CT} , and m_{CT2} [15–32].

While these methods work well under idealized conditions, in practice there can be serious obstacles to implementing them successfully. Perhaps the most important problem, common to all these approaches, is the presence of combinatoric backgrounds which occur because the new particles must be produced in pairs. For example, consider the process where two gluinos are produced and decay through a squark to a neutralino: $\tilde{g}\tilde{g} \rightarrow qq\tilde{\chi}_1^0\tilde{\chi}_1^0$. We will observe four jets, but we do not know which were emitted first nor from which gluino

each was emitted. There is thus an ambiguity in reconstructing the event from the visible particles; we will refer to this as a combinatorial ambiguity. In general, with pair-produced parents that decay via identical long cascades, combinatorial ambiguities present a major hurdle in distinguishing the appropriate assignment of particles to each chain as well as the unique ordering of these particles, as discussed in a recent review on mass reconstruction techniques [30]. Wrong assignments can lead to significant suppression of mass peaks and cause large tails in distributions [14]. We also note that understanding these ambiguities is crucial in extracting the nature of the new physics.

We emphasize that these kinematic reconstruction methods are not affected equally by wrong combinations. In fact, the most general transverse variable based on m_{T2} , known as m_{TGen} [17], does not suffer from combinatorial ambiguities since it explicitly includes a minimization over all possible decay chain assignments of the observed object momenta. For regular m_{T2} studies, the assignment ambiguity, *i.e.* assigning particles to separate decay chains, is relevant, while the ordering ambiguity, *i.e.* the sequence of the particles on the decay chain, is not important: by construction, the transverse mass of each decay chain is irrespective of decay chain placement, but is clearly dependent on decay chain assignments. The subsystem m_{T2} reconstruction method [24, 26], however, is adversely affected by both the assignment ambiguity and the ordering ambiguity. Similarly, wrong assignment combinations and wrong ordering choices degrade the effectiveness of the polynomial method [10, 13, 14] and can also worsen results from the kinematic edges approach if the invariant mass distributions do not encapsulate entire decay chains.

In this paper, we will focus on resolving the combinatorial ambiguity arising from decay chain assignments, leaving the question of resolving ordering ambiguities for the future. Thus, our results should improve the effectiveness of all of the aforementioned kinematic reconstruction methods except m_{TGen} , which, as noted above, does not suffer from assignment ambiguities. Henceforth, “combinatorial ambiguity” will refer solely to the decay chain assignment ambiguity discussed above.

In previous kinematic reconstruction studies, past authors have designed a variety of methods to address combinatorial ambiguities. For example, in [13, 14], they apply the polynomial method to pairs of events, and they address combinatorial ambiguities by favoring, for a given event, the assignment that maximizes the number of event pairings that give algebraic solutions. In this way, they hoped to discard wrong combinations of a given event

that would give unphysical solutions when paired with correct combinations of other events. In [31], which used m_{T2} - and sub-system m_{T2} -based methods, they chose the combinations of jet pairs with smaller invariant masses and smaller angular separation as well as discarding the largest sub-system m_{T2} values, arguing that correct jet pairings should be directionally focused, and high invariant mass jet pairings are more likely incorrect. While these representative approaches at reducing wrong combinations work on an individual analysis basis, we note that these methods are not interchangeable. Even though the combinatorial ambiguity for kinematic reconstruction studies is in general a common difficulty, many of the specific approaches to resolve such combinatorial ambiguities used in the literature cannot be generalized when using more than one kinematic reconstruction technique.

One exception is the hemisphere method, used in [21, 22, 24, 29] (we will describe this method in detail below in Sec. III). If the parent particles of each decay chain are strongly boosted, their decay products will be collimated along the initial momenta. By considering events with suitably large transverse momenta, one may hope to avoid combinatorial ambiguities (cf. Sec. 13.4 of [33]). However, this can lead to significant loss in signal statistics. On the other hand, the hemisphere method of reducing combinatorial ambiguities allows for the simultaneous application of multiple kinematic reconstruction methods, without a specialized approach.

In this paper, we present a new method for resolving such combinatorial ambiguities in decay chains. Our method is described in Sec. IV. We show that our method can yield highly accurate assignments of particles to decay chains which have little contamination from wrong combinations. We contrast our method with a parallel study of the efficacy of the more familiar hemisphere method. Our results show that for cascade decay chains with on-shell mass resonances, our method improves signal retention up to a factor of 2 over the usual hemisphere method.

We begin by presenting two toy models, which we shall use to compare the two methods. In Sec. II, we present the model masses and aspects of the simulation. In Sec. III, we review the hemisphere method and give our hemisphere method implementation details. We then discuss our new method (which we shall call the p_T v. M method) in Sec. IV and describe the specifics of our procedure in Sec. V. We compare the two methods in Sec. VI and conclude in Sec. VII.

Model Name	\tilde{g} (GeV)	\tilde{q} (GeV)	$\tilde{\chi}_1^0$ (GeV)	Diquark Invariant Mass edge (GeV)
Model A	600	400	100	433
Model B	600	800	100	500

TABLE I. Model spectra.

II. MODELS

In this section, we present the toy models used in our analysis. The masses of the two models considered are summarized in Table I. Roughly, Model A mimics a SPS1a-style mass spectrum, while Model B represents an off-shell squark scenario.

Our aim is to isolate the combinatorial ambiguities arising from pure signal events when the final state particles are indistinguishable inside the detector. We focus solely on gluino pair production with each gluino decaying to the lightest neutralino and two quarks: $\tilde{g}\tilde{g} \rightarrow qq\tilde{\chi}_1^0\tilde{\chi}_1^0$. The intermediate squark is on-shell (Model A) or off-shell (Model B). All quarks are treated at parton level, and effects from initial state radiation or parton showering are not considered. These events have three distinct pair-pair combinations. Isolating which particles arise from the same decay chain is a first step in any kinematic event analysis. Since we are tackling the combinatorial ambiguity that arises even when dealing with only signal events, we shall not complicate our analysis by adding background events or multiple production or decay modes.

It is well known that cascade decays impose restrictions on the kinematics of the outgoing decay products. For our gluino cascade decay, the diquark invariant mass edge for on-shell intermediate squarks is

$$m_{qq}|_{\text{edge}} = \sqrt{\frac{(m_{\tilde{g}}^2 - m_{\tilde{q}}^2)(m_{\tilde{q}}^2 - m_{\tilde{\chi}_1^0}^2)}{m_{\tilde{q}}^2}}, \quad (1)$$

assuming the quarks are massless, and where $m_{\tilde{g}}$, $m_{\tilde{q}}$, and $m_{\tilde{\chi}}$ are the mass of the gluino, squark, and neutralino, respectively. For the off-shell squark case, the edge value is simply

$$m_{qq}|_{\text{edge}} = m_{\tilde{g}} - m_{\tilde{\chi}_1^0}. \quad (2)$$

Of necessity, a correct assignment of the jets to the two sides of the event will have the invariant mass of the jet-jet pair below the kinematic edge. Naturally, an incorrect pair

assignment can produce an invariant mass beyond the relevant kinematic edge, since the two quarks are uncorrelated. Also, note that the diquark invariant mass distribution through an on-shell squark possesses a characteristic triangular shape, with its rising edge saturating the upper endpoint. On the other hand, the off-shell squark case has the upper invariant mass edge characteristically falling near the endpoint. Thus, the kinematic edge is easier to identify in on-shell scenarios, and in either case, rejection of pair assignments with invariant masses beyond the edge serves to reduce combinatorial ambiguities.

Having defined our models, we now try and resolve combinatorial ambiguities in these models. We used MadGraph/MadEvent 4.4.26 [34] to generate 100,000 events of pair-produced gluinos at masses of 600 GeV with a 7 TeV and 14 TeV LHC without initial state radiation. Using BRIDGE 2.18 [35], we force these gluinos to decay to the lightest neutralino through an on-shell or off-shell squark. We do not simulate any direct squark pair production or squark-gluino associated production.

III. THE HEMISPHERE METHOD

The hemisphere method attempts to delineate two hemispheres in an event, whereby all objects in a given hemisphere are ideally from the same decay chain. The rationale for this method is the assumption that hard scattered parent particles are approximately back-to-back in the lab frame. This is not quite correct in hadron colliders because the longitudinal parton momenta of the initial state cannot be tuned. The hope is, however, that the parent particles give a large boost to their separate decay chains, and so a given cone or hemisphere for each parent particle will generally capture all of their daughter particles.

In practice, the hemisphere method is implemented as a two-step process. First, one chooses two seeds that will serve as the starting object for each side of the event. Second, one clusters the remaining objects according to some figure of merit with one seed or the other. This figure of merit is typically taken to be pdR , where $p \equiv |\Delta(\vec{p})|$ is the magnitude of the three-momentum difference between the object and a given seed and $dR \equiv \sqrt{(\Delta\phi)^2 + (\Delta\eta)^2}$ is roughly the angular separation: the object is clustered with whichever seed minimizes pdR .

One also needs some method for choosing the seeds. In our analysis, we adopt the traditional method of choosing the highest p_T object to be the first seed. For the second seed, following the treatment in Sec. 13.4 of [33], we choose either (**PDR1**) the object that

maximizes pdR relative to the first seed or (**PDR2**) the object that maximizes the invariant mass of the pair. With these two seeds, we then calculate the pdR value of the object with respect to each seed, and we cluster the object to be with seed 1 or seed 2 according to which seed minimizes the produced pdR .

We note that since we have four quarks in each event, we have a possibility of an assignment where one seed is by itself and three quarks are assigned to the other side; we will refer to these as singlet-triplet assignments. These are all incorrect assignments, since the proper partition of the event in the particular case we are considering requires two quarks assigned to each side. Though these events do contain useful kinematic information, we choose to discard them for simplicity.

We implement selection cuts at each stage of seed selection and object clustering. These cuts are summarized as follows:

- Cut 1: The p_T of the initial seed quark (the highest p_T object in the event) must be at least 200 GeV.
- PDR1 Cut 2: The minimum pdR between seed 1 and seed 2 must be 1800 GeV.
- PDR2 Cut 2: The invariant mass M between seed 1 and seed 2 must be greater than the theoretically calculated diquark kinematic edge value (we assume this can be experimentally measured accurately).
- Cut 3: We discard all singlet-triplet events, ensuring that we work with events that have been divided into pair-pair combinations.
- Cut 4: We impose the restriction that the maximum seed-object invariant mass is the theoretical diquark kinematic edge value, calculated from Eq. (1) and Eq. (2).

The cut efficiency, which is the percentage of all events that survive cuts, is summarized in Table II for the above cuts.

Finally, one can place a cut on the difference of the two values of pdR calculated for each object with respect to the two seeds. The rationale is that if the pdR between an object and seed 1 is much smaller than the corresponding pdR value with respect to seed 2, then it is more likely that the object is associated with seed 1. By making the minimum required difference of these two pdR values larger, the probability of an incorrect assignment can be reduced, at the cost of losing signal events. We therefore adopt a variable cut that progressively obtains higher event purity at the expense of decreasing event efficiency, which

	PDR1				PDR2			
Model Name	Cut 1	Cuts 1-2	Cuts 1-3	Cuts 1-4	Cut 1	Cuts 1-2	Cuts 1-3	Cuts 1-4
Model A - 7 TeV	78.8%	25.2%	12.4%	12.2%	78.8%	51.4%	26.1%	25.7%
Model A - 14 TeV	81.7%	35.8%	18.5%	18.2%	81.7%	58.1%	30.5%	30.1%
Model B - 7 TeV	81.8%	27.1%	13.4%	13.3%	81.8%	38.5%	19.6%	19.6%
Model B - 14 TeV	83.9%	37.5%	19.2%	18.7%	83.9%	46.1%	24.4%	24.4%

TABLE II. Efficiencies for PDR1 and PDR2 cuts.

will serve as a performance measure for later comparison.

- We change the minimum difference in pdR in order for an object to be assigned to a given seed from 0 to 2000 GeV.

IV. THE p_T V. M METHOD

Our method is similar in spirit to the hemisphere method, but it is more flexible, more model-independent, and performs better for on-shell cascade decay chains. We have already seen that considering cuts in invariant mass (i.e. considering events below the diquark edge) can reject some wrong combinations. On the other hand, the hemisphere method takes advantage of large p_T boosts to help separate hemispheres and reduce ambiguities. Our goal is to combine these ideas; simply stated, we look for correlations in high transverse momentum pairs with low invariant mass.

We begin by considering Model A at a 7 TeV pp collider. We generate a large number of events as described above, and plot all diquark combinations (both correct and incorrect assignments) according to their summed p_T and invariant mass M , in Fig. 1. Considering the left panel and neglecting the shading for the moment, we notice two prominent features. The first is the kinematic edge in the invariant mass, especially visible for high p_T ; as we move towards large invariant mass at high p_T , the number of combinations drops off beyond a certain invariant mass. This is just a new way of seeing that correct diquark assignments must all lie below the kinematic edge, while incorrect assignments can have much larger values of invariant mass, producing an excess of events at lower invariant mass. Correspondingly, the excess of diquark combinations with invariant mass larger than the edge value must all

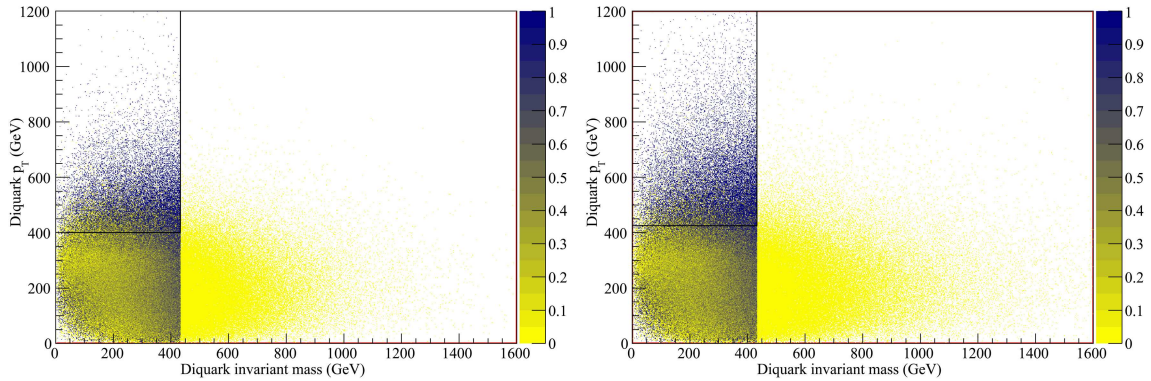


FIG. 1. (color online). (A) Model A - 7 TeV; (B) Model A - 14 TeV - Diquark transverse momentum $v.$ invariant mass, correct and wrong combinations. The shading of the point reflects the fraction of correct combinations according to the key on the right. The boxes of (A) $p_T > 400$ GeV and $M_{qq} \leq 433$ GeV and (B) $p_T > 425$ GeV and $M_{qq} \leq 433$ GeV indicate regions with (A) 91.9% event purity and 5.7% event efficiency; (B) 95.7% event purity and 7.2% event efficiency.

be wrong combinations.

We also recognize a second feature; as we increase p_T , there is again an excess in the diquark combinations below the kinematic edge. This is particularly noticeable if we only look at the events which have invariant masses larger than the kinematic edge (which are all incorrect combinations). These events tail off quickly towards higher p_T , while events below the kinematic edge (a mixture of correct and incorrect combinations) extend to higher p_T . A natural guess (based on the success of the hemisphere method) is that the combinations at large p_T are dominated by correct assignments. Roughly, we expect correct combinations to carry higher p_T than wrong combinations because correct combinations share the same transverse momentum of the parent gluino in the lab frame, while wrong combinations should generically have canceling parent gluino transverse momenta.

We have used our knowledge of the parton-level information to shade Fig. 1 according to the percentage of diquark pairs at each p_T $v.$ M point that are correct. We see explicitly that the correct and incorrect combinations occupy distinct regions of this plot; the correct combinations characteristically have larger p_T and lower invariant masses. Moreover, as we increase to a 14 TeV LHC, we expect the population of high p_T correct combinations to increase, because of the higher boost of the parent particles, as depicted in the right panel

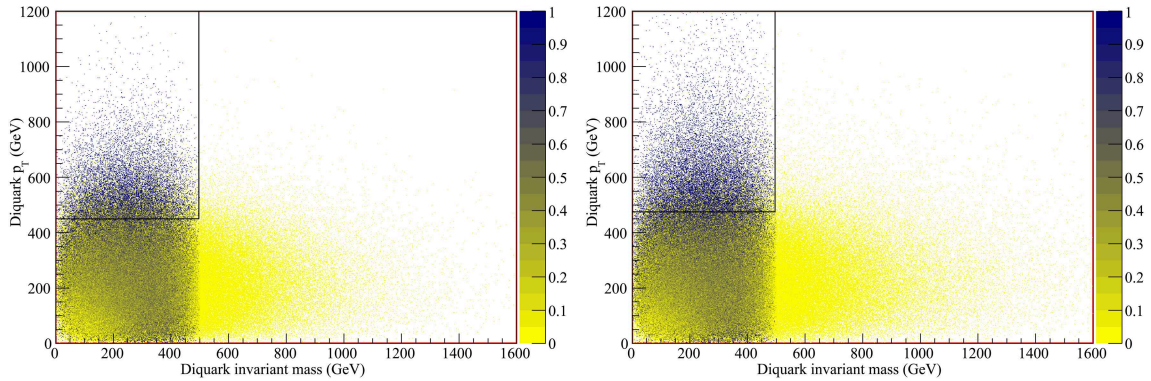


FIG. 2. (color online). (A) Model B - 7 TeV; (B) Model B - 14 TeV - Diquark transverse momentum $v.$ invariant mass, correct and wrong combinations. Same shading scheme as Fig. 1. The boxes of (A) $p_T > 450$ GeV and $M_{qq} \leq 500$ GeV and (B) $p_T > 475$ GeV and $M_{qq} \leq 500$ GeV indicate regions with (A) 91.7% event purity and 3.1% event efficiency; (B) 94.4% event purity and 4.2% event efficiency.

of Fig. 1. Similar results are also evident for Model B, as seen in Fig. 2.

This strongly suggests that a cut on combinations with invariant mass below the kinematic edge and high p_T can guarantee an event sample dominated by correct combinations. We now present a practical method for performing this cut.

V. THE p_T V. M PROCEDURE

Given an event with four quarks, we implement our method according to the following procedure:

1. For each event, plot the p_T and M of each diquark pair (all six pairings).
2. Isolate the diquark invariant mass edge M_0 . This is usually immediately visible as a cutoff at larger invariant masses.
3. Now only consider the pairs with invariant mass larger than the kinematic edge. Choose a p_T threshold value P_0 such that fewer than 5% of these pairings have p_T larger than this threshold value. For example, in Model A at a 7 TeV LHC, this corresponds to a threshold value of about 400 GeV.
4. For each event, we require that there be a division of the 4 quarks into two pairs

such that the p_T of each pair is larger than P_0 , and the invariant mass of each pair is below M_0 . If there is no such division possible or if more than one division is possible, we discard the event. If exactly one division passing the requirement is possible, the event is retained and the assignment which passes the cut is treated as the proper assignment of the quarks to the two sides.

We note that neither the p_T cut nor the invariant mass cut we have chosen have been optimized. Choosing a higher P_0 would generally ensure a purer event sample with fewer incorrect combinations; however, a higher P_0 also reduces signal statistics. Finding an optimum balance between event purity and signal statistics will be a model-dependent, search channel-dependent question. Moreover, this procedure is readily extended to more complicated event signatures, such as multi-jet and multi-lepton events, and can also be used as a figure of merit to cluster entire sides all at once.

VI. COMPARISON OF METHODS

In this section, we present a comparison between the hemisphere method and our new p_T v. M method. We will use event purity against event efficiency as a comparison measure. We will define event purity as the percentage of events where the quarks of the event are paired correctly. Event efficiency is defined as the percentage of total events that pass the imposed cuts.

We can benchmark the performance of the hemisphere method and the p_T v. M method by adjusting cuts. For the hemisphere method, increasing the minimum difference in pdR in order for an object to be assigned to a seed makes it more likely that a given object and seed are from the same decay chain. For the p_T v. M method, we can increase the success of isolating the correct pair-pair combination by increasing the p_T cut on each pair of a pair-pair combination.

In Fig. 3, we show the event purities as a function of event efficiencies for Model A with a 7 TeV and 14 TeV LHC. For this on-shell mass spectrum, we can readily see that the p_T v. M method delivers far better event efficiency for a given event purity than either PDR1 or PDR2. For 85% purity, the Model A - 7 TeV event sample from p_T v. M is approximately twice as large as either hemisphere method sample. While the difference in performance is moderately reduced for a 14 TeV LHC, the superiority in performance is still impressive. At

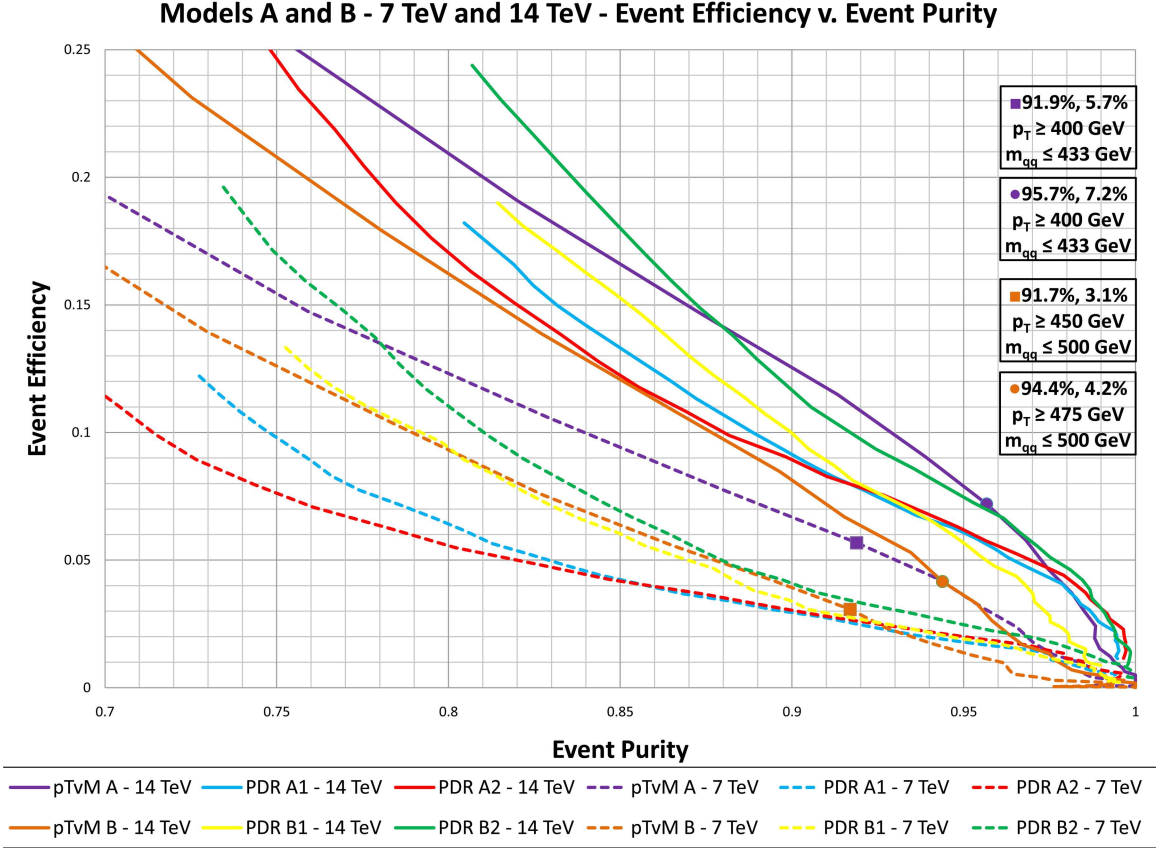


FIG. 3. (color online). Models A and B - Event purity v. efficiency, as defined in the text. The marked points of (91.9%, 5.7%) and (95.7%, 7.2%) for Model A and (91.7%, 3.1%) and (94.4%, 4.2%) for Model B correspond to the outlined boxes in Fig. 1 and Fig. 2, respectively.

90% purity, for example, the p_T v. M event sample is about 33% more. From our earlier procedure given in Sec. V, where the survival rate of wrong diquark pairings in the region to the right of the invariant mass edge was about 5%, we obtain the two marked points of (91.9%, 5.7%) for Model A - 7 TeV and (95.7%, 7.2%) for Model A - 14 TeV.

For the off-shell scenario, also shown in Fig. 3, the performance for all three methods is approximately the same at a 7 TeV LHC. A 14 TeV LHC, however, shows the PDR2 method performing best, with a 50% gain in event efficiency over the p_T v. M method for 85% event purity. The difference is greater for higher purities, becoming approximately 100% for 95% purity. Using the procedure of Sec. V with a survival rate of about 5%, we find the points (91.7%, 3.1%) and (94.4%, 4.2%) for Model B - 7 TeV and 14 TeV, respectively. While good purity can be obtained for off-shell models using the p_T v. M method, the hemisphere method is better. We can hypothesize that the hemisphere methods work better in the

off-shell case because the directionality of the diquark pairs is roughly uniform. Because the hemispheres created using pdR can lie in an arbitrary orientation with respect to the beam axis, they are more flexible in capturing the correct diquark pairings than the p_T v. M method, which necessarily requires the two quarks to have lots of momenta in the plane transverse to the beam axis. When the intermediate squark is on-shell, however, the squark typically gives a large boost to the second emitted quark, which helps result in a high p_T diquark pair. From the plots, we thus observe that the traditional pdR method of assigning particles to decay chains seems well-suited for off-shell decays, but is significantly outperformed by our new p_T v. M method for on-shell cascade decays.

VII. CONCLUSION

We have compared the performance of the hemisphere method with the p_T v. M method using the models presented in Table I. We have shown the p_T v. M selection criteria of Sec. V delivers $\mathcal{O}(25\%)$ to $\mathcal{O}(100\%)$ more event statistics for a given purity between 85% to 95% than the traditional pdR methods for an on-shell decay chain. This is a substantial increase in the number of viable signal events and would be a useful method for any study that suffers from decay chain assignment combinatorial ambiguities. The hemisphere method, on the other hand, seems well-suited for off-shell decay chains. A realistic collider study should benefit from adopting both methods in parallel, since it is not generally known beforehand whether the observed decay products are produced on-shell or off-shell. One possibility for improving the off-shell performance of p_T v. M is to salvage the events with more than one combination (not “pure”) by retaining only the pair-pair combination that has the largest scalar total p_T . This is left for future work.

We remark that although this study was performed using simplified models without detector effects, ISR/FSR, or background simulation, we believe the major features of our results are retained when going to full models. As an important validation, our hemisphere method performance results are qualitatively similar to those presented in Sec. 13.4 of [33], which used a CMS detector simulation. At high LHC energies, however, the effects of ISR is clearly not negligible, especially when the ISR jet gives a large p_T boost to the entire hard process. In such scenarios, we would expect the additional ISR jet to adversely degrade both efficiency and purity of retained signal events. We expect the effect to be similar to both

the hemisphere method and the p_T v. M method, though, since the inclusion of a large p_T ISR jet makes the remaining jets more isotropic. We are currently studying possible implementations of the p_T v. M method to tag events with large p_T ISR jets and potentially tag ISR jets.

One drawback of our method is the assumed observation of the dijet invariant mass edge. While we do not prescribe an exact method to extract this edge largely because of jet energy scale uncertainties, our method highlights the fact that wrong combinations (which can pollute and exceed the edge value) can be removed with moderate dijet p_T cuts, perhaps allowing a more accurate extrapolation of the edge value if one understands the expected shape of the resulting invariant mass distribution. Moreover, mass measurements initially will focus on dilepton invariant mass edges, which are relatively straightforward to observe given the good understanding of lepton kinematics in detectors. We envision that once dilepton edges are measured, the p_T v. M method could be used to isolate any available dilepton+jet and dilepton+dijet edges; given this information, the edge in the dijet cross channel could be extracted and further kinematic studies in multi-jet final states would proceed given the relatively pure signal samples determined from the p_T v. M method.

A separate issue is that our on-shell Model A spectrum, which was chosen to mimic the SPS1A benchmark point, gives distinct, highly energetic jets. If the jets were less energetic, reflecting a compressed SUSY spectrum, (for example, $\tilde{g} = 600$ GeV, $\tilde{q} = 500$ GeV, and $\tilde{\chi}_1^0 = 400$ GeV) we would find that the p_T v. M method performs approximately as well as the hemisphere method at a 7 TeV LHC and slightly worse (about 15%–25% less efficient) for a 14 TeV LHC, but the overall efficiency is increased by a factor of 2 for the p_T v. M method. For compressed spectra, we thus see the relative performance of the p_T v. M method matches that presented for the off-shell Model B spectrum.

We expect the p_T v. M method to be useful for other signatures besides the one presented in this study, since we are taking advantage of kinematic features found in all cascade decay chains. It is straightforward to consider combinatorial ambiguities arising from multi-lepton or leptons+jets final states. Additionally, we could extend our method to resolve ambiguities when the final state includes heavy, reconstructed W or Z gauge bosons with minor modifications to the expected invariant mass spectrum. One main difficulty with such a generalization, however, is multiple branching modes occur with similar kinematics, such as a gluino decay via multiple on-shell squark modes where the squarks are largely degenerate.

Here, the signal-only combinatorial ambiguity among light jets is shared among multiple decay modes, and because the observed kinematics are similar, it will be difficult to apply kinematic cuts to distinguish distinct decay chains. We are currently in the process of applying this method to analyze new physics models passing through a realistic detector simulation. In particular, a study of precision determination of invariant mass edges including dilepton and dijet edges at the SPS1A benchmark point is underway and seeks to demonstrate the usefulness of this method in a collider environment.

A further direction of research is to improve the p_T v. M method, for example by performing a shape analysis of the correct vs. wrong combinations in the p_T v. M plane in order to optimize the p_T v. M cut. It may also be possible to implement the p_T v. M method on an event-by-event basis, for example, by preferentially choosing pair-pair combinations at the event level according to the maximum p_T/M or another similar figure of merit. Such a measure may be superior to the pdR method for off-shell decay scenarios. Finally, we would also want to study how our method can be applied to improve the determination of the overall mass scale and the LSP/LKP mass at colliders. We hope to return to these issues in future work.

ACKNOWLEDGEMENTS

FY is supported by an LHC Theory Initiative Graduate Fellowship, NSF Grant No. PHY-0705682. AR and FY are supported by NSF Grant No. PHY-0653656 and PHY-0970173.

-
- [1] H. Baer, C. h. Chen, F. Paige and X. Tata, Phys. Rev. D **52**, 2746 (1995) [arXiv:hep-ph/9503271].
 - [2] I. Hinchliffe, F. E. Paige, M. D. Shapiro, J. Soderqvist and W. Yao, Phys. Rev. D **55**, 5520 (1997) [arXiv:hep-ph/9610544].
 - [3] H. Baer, C. h. Chen, M. Drees, F. Paige and X. Tata, Phys. Rev. D **59**, 055014 (1999) [arXiv:hep-ph/9809223].
 - [4] I. Hinchliffe and F. E. Paige, Phys. Rev. D **60**, 095002 (1999) [arXiv:hep-ph/9812233].
 - [5] H. Bachacou, I. Hinchliffe and F. E. Paige, Phys. Rev. D **62**, 015009 (2000) [arXiv:hep-ph/9907518].

- [6] I. Hinchliffe and F. E. Paige, *Phys. Rev. D* **61**, 095011 (2000) [arXiv:hep-ph/9907519].
- [7] B. C. Allanach, C. G. Lester, M. A. Parker and B. R. Webber, *JHEP* **0009**, 004 (2000) [arXiv:hep-ph/0007009].
- [8] J. Hisano, K. Kawagoe, R. Kitano and M. M. Nojiri, *Phys. Rev. D* **66**, 115004 (2002) [arXiv:hep-ph/0204078].
- [9] J. Hisano, K. Kawagoe and M. M. Nojiri, *Phys. Rev. D* **68**, 035007 (2003) [arXiv:hep-ph/0304214].
- [10] M. M. Nojiri, G. Polesello and D. R. Tovey, arXiv:hep-ph/0312317.
- [11] K. Kawagoe, M. M. Nojiri and G. Polesello, *Phys. Rev. D* **71**, 035008 (2005) [arXiv:hep-ph/0410160].
- [12] H. C. Cheng, J. F. Gunion, Z. Han, G. Marandella and B. McElrath, *JHEP* **0712**, 076 (2007) [arXiv:0707.0030 [hep-ph]].
- [13] H. C. Cheng, D. Engelhardt, J. F. Gunion, Z. Han and B. McElrath, *Phys. Rev. Lett.* **100**, 252001 (2008) [arXiv:0802.4290 [hep-ph]].
- [14] H. C. Cheng, J. F. Gunion, Z. Han and B. McElrath, *Phys. Rev. D* **80**, 035020 (2009) [arXiv:0905.1344 [hep-ph]].
- [15] C. G. Lester and D. J. Summers, *Phys. Lett. B* **463**, 99 (1999) [arXiv:hep-ph/9906349].
- [16] A. Barr, C. Lester and P. Stephens, *J. Phys. G* **29**, 2343 (2003) [arXiv:hep-ph/0304226].
- [17] C. Lester and A. Barr, *JHEP* **0712**, 102 (2007) [arXiv:0708.1028 [hep-ph]].
- [18] W. S. Cho, K. Choi, Y. G. Kim and C. B. Park, *Phys. Rev. Lett.* **100**, 171801 (2008) [arXiv:0709.0288 [hep-ph]].
- [19] B. Gripaios, *JHEP* **0802**, 053 (2008) [arXiv:0709.2740 [hep-ph]].
- [20] A. J. Barr, B. Gripaios and C. G. Lester, *JHEP* **0802**, 014 (2008) [arXiv:0711.4008 [hep-ph]].
- [21] W. S. Cho, K. Choi, Y. G. Kim and C. B. Park, *JHEP* **0802**, 035 (2008) [arXiv:0711.4526 [hep-ph]].
- [22] M. M. Nojiri, Y. Shimizu, S. Okada and K. Kawagoe, *JHEP* **0806**, 035 (2008) [arXiv:0802.2412 [hep-ph]].
- [23] D. R. Tovey, *JHEP* **0804**, 034 (2008) [arXiv:0802.2879 [hep-ph]].
- [24] M. M. Nojiri, K. Sakurai, Y. Shimizu and M. Takeuchi, *JHEP* **0810**, 100 (2008) [arXiv:0808.1094 [hep-ph]].
- [25] H. C. Cheng and Z. Han, *JHEP* **0812**, 063 (2008) [arXiv:0810.5178 [hep-ph]].

- [26] M. Burns, K. Kong, K. T. Matchev and M. Park, *JHEP* **0903**, 143 (2009) [arXiv:0810.5576 [hep-ph]].
- [27] A. J. Barr, B. Gripaios and C. G. Lester, *JHEP* **0911**, 096 (2009) [arXiv:0908.3779 [hep-ph]].
- [28] W. S. Cho, J. E. Kim and J. H. Kim, arXiv:0912.2354 [hep-ph].
- [29] S. G. Kim, N. Maekawa, K. I. Nagao, M. M. Nojiri and K. Sakurai, *JHEP* **0910**, 005 (2009) [arXiv:0907.4234 [hep-ph]].
- [30] A. J. Barr and C. G. Lester, arXiv:1004.2732 [hep-ph].
- [31] M. Blanke, D. Curtin and M. Perelstein, *Phys. Rev. D* **82**, 035020 (2010) [arXiv:1004.5350 [hep-ph]].
- [32] W. S. Cho, W. Klemm and M. M. Nojiri, arXiv:1008.0391 [hep-ph].
- [33] G. L. Bayatian *et al.* [CMS Collaboration], *J. Phys. G* **34**, 995 (2007).
- [34] J. Alwall *et al.*, *JHEP* **0709**, 028 (2007) [arXiv:0706.2334 [hep-ph]].
- [35] P. Meade and M. Reece, arXiv:hep-ph/0703031.